Mapping the binding motifs of deprotonated monounsaturated fatty-acids and their corresponding methyl esters within supramolecular capsules

Kaiya Wang, Bruce C. Gibb*

Department of Chemistry
Tulane University
New Orleans, LA 70118, USA
bgibb@tulane.edu

Table of Contents



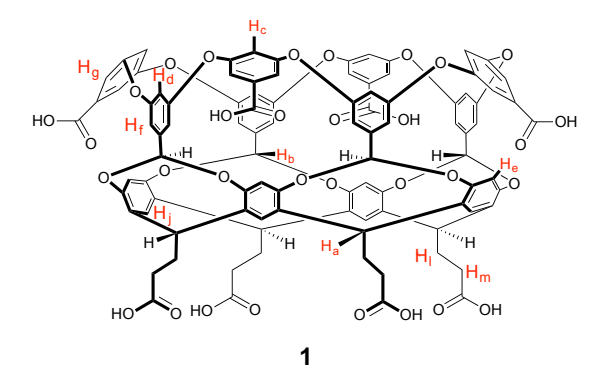
Abstract

A suite of NMR techniques revealed that cavitand (1) formed 2:1 host-guest complexes with a range of mono-unsaturated fatty carboxylates and their corresponding methyl esters. All of the carboxylates bound to the capsule in a J-shaped motif with the carboxylate at the equatorial region of the dimeric capsule, and the reverse turn of the chain and the methyl terminal in each polar region of the host. Guest exchange was slow on the NMR timescale, whilst tumbling was slow or close to the NMR timescale depending on the position and stereochemistry of the double bond. In contrast, the methyl esters were found to bind in three motifs depending on the position and stereochemistry of the double bond. Thus the esters were observed to bind in either a J-shaped, U-shaped (the turn in the guest occupying a polar region and the two termini competing for occupancy of the other pole), or a reverse J-shaped motif (ester moiety and turn each occupying a pole and the methyl terminal located near the equator). Relative binding constants (K_{rel}) determinations revealed that the affinity for the capsule was dependent on the position and stereochemistry of the double bond.

Introduction

Understanding molecular behavior within yocto-liter compartments can offer new perspectives on biological phenomena in Nature, and open the way to highly unusual and selective forms of catalysis,¹⁻⁹ as well as molecular protection¹⁰⁻¹³ and separation strategies.^{14,15}

We have previously reported on the kinetic resolution of constitutionally isomeric esters using the dimeric capsule formed by octa-acid **1** in basic media. In the absence of the host the selected guests revealed the expected relationship between their hydrolysis rates and the size of their alkoxy R group. However, in the presence of the host these intrinsic reaction rates were strongly modulated by the affinity that each ester had for the dry yocto-liter environment of the capsule. Hence by this type of selective molecular protection it was possible to bring about the kinetic resolution of pairs of esters that otherwise couldn't be separated by selective hydrolysis in free solution.



Key to all of these applications within yocto-liter compartments is the preferred conformation and orientation of the bound guest (its packing motif). In the aforementioned case of ester resolution the guests were relatively small compared to the overall capacity of the host, and these and other studies using fully capsular hosts have revealed that at such low packing coefficients highly flexible molecules adopt principally extended motifs with *anti* dihedral angles down the length of the main-chain of the guest. These same studies also revealed that when packing is more constrained helical motifs with *gauche* conformations along the chain are found to predominate. This is an unlikely conformation within free solution, but the opportunity to make more contacts with the walls of the capsule more than compensates. As the alkane or alkyl chain is increased in length further relative to the capsule length, this motif becomes untenable. Instead guests adopt U-shaped or J-shaped motifs with a reverse turn located within the chain. Similar higher-energy U- or J-shaped motifs have also been observed in fatty acids bound to their proteinaceous transporters, and with bolaamphiphiles bound to bowl-shaped hosts and more open cucurbiturils. Building on these findings, very recent results have shown how controlling such conformations can be used to template cyclization

reactions.26,28,29

Considering our early successes with the kinetic resolution of carboxylic esters using octa-acid **1**, we wished to examine analogous kinetic resolutions of long-chain fatty acid esters (Figure 1).³⁰⁻³³ There are three principal reasons for this. First, as structural components of bilayers, as energy sources, and as signaling molecules,³⁴ fatty acids and their esters play vital roles in biology and health.³⁵ Second, the separation of fatty acids and esters differing only in the location or stereochemistry of a sole double bond is frequently problematic.³⁶ Third, we envisaged that the position and stereochemistry of the C=C double bonds in these molecules would significantly influence their packing motif within the confines of the dimer of **1**, and hence the outcome of corresponding kinetic resolution experiments.

As a first step towards examining the kinetic resolution of these fatty acid esters, we report here on the binding of esters **2a-12a** (Figure 1) and their corresponding free carboxylates (**2b-12b**) to the dimer formed by **1**. Our results show that changes to the head group (carboxylate or ester) and the position and stereochemistry of the double bond all greatly influence the affinity, packing motif, and mobility of a guest within the capsule.

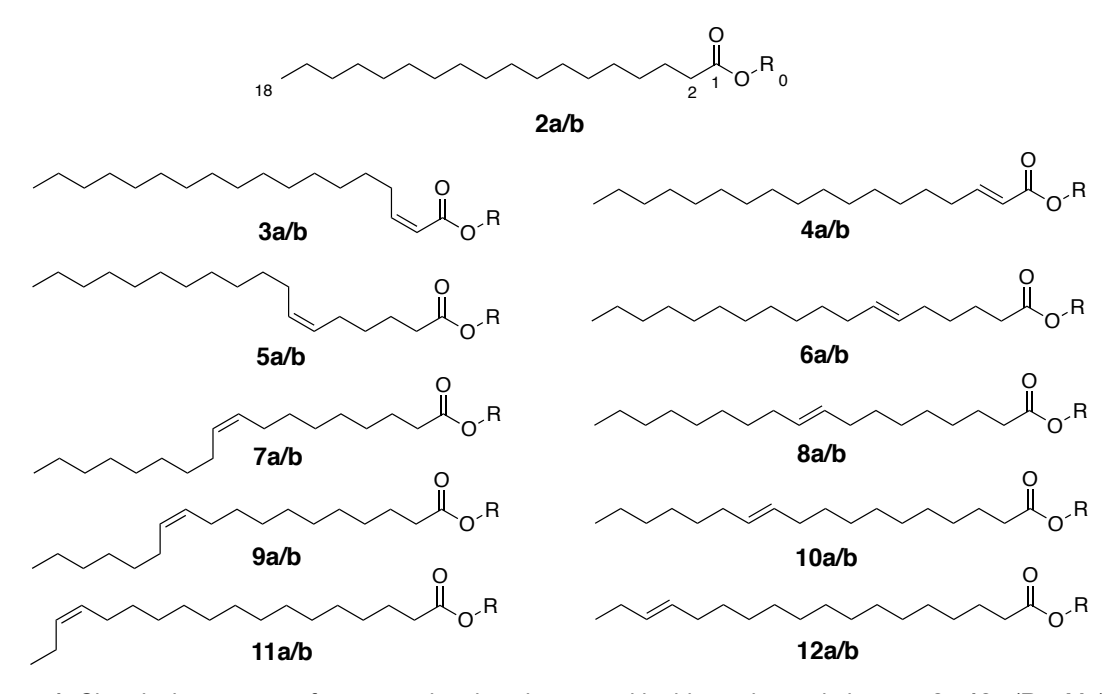


Figure 1: Chemical structures of esters and carboxylates used in this study: methyl esters 2a-12a (R = Me) and sodium carboxylates 2b-12b (R = Na). Atom numbering used in this study is shown in structure 2a/b.

Results and Discussion

The host central to this study is octa-acid deep-cavity cavitand **1**. ^{37,38} Under basic conditions octa-acid is capable of binding a broad range of amphiphilic^{39,40} and anionic^{41,42}

guests as 1:1 host-guest complexes, or forming capsular 2:1 (or 2:2) host-guest complexes with more non-polar guests.⁴³ Driven by the Hydrophobic Effect,^{44,45} host **1** forms capsular complexes with guests as large as those possessing twenty-seven non-hydrogen atoms,³⁷ and consequently it was expected that it would readily form 2:1 complexes with the methyl esters used in this study. This was also suggested by recent work that included the 2:1 capsular complex between **1** and stearic acid/stearate **2b**.⁴⁶

Guest Synthesis

Among the esters studied here, saturated ester **2a** and six of the mono-unsaturated derivatives (**5a-10a**) were commercially available. Esters **3a**, **4a**, **11a** and **12a**, were synthesized by Wittig chemistry (Scheme 1 and Scheme 2 and Supporting Information).⁴⁷ Specifically, compounds **3a** and **4a** were accessed by forming the triphenyl phosphonium salt of 1-bromopentadecane and reacting its ylide (formed with sodium *bis*(trimethylsilyl)amide) with methyl 2-oxoacetate (Scheme 1). This gave a 60:40 ratio of the two stereoisomers that were separated by column chromatography.

Scheme 1: Synthesis of guests 3a and 4a.

Ester **11a** was obtained (Scheme 2) by converting 15-hydroxypentadecanoic acid to its methyl ester, oxidation of the terminal hydroxy group to the corresponding aldehyde, and treatment of this with the ylide formed by reacting propyltriphenylphosphonium bromide and sodium *bis*(trimethylsilyl)amide. This process led to only trace amounts of ester **12a**, and as a result this *trans*-isomer was obtained via a two-step epoxidation/elimination interconversion of **11a**.⁴⁸

Scheme 2: Synthesis of guests 11a and 12a.

Except where specifically required (*vide infra*), the different acids were synthesized as their complexes within the octa-acid **1** dimer by simply treating the corresponding ester complex with excess NaOH.

Sodium carboxylates 3b-12b binding to octa-acid 1

The binding of stearic acid/stearate **2b** (Figure 1) and five other saturated acids to the dimer capsule $\mathbf{1}_2$ has been reported previously. This study revealed that the acid guests formed a stable 2:1 host-guest complex but that shorter chained guests formed weaker, faster-exchanging complexes. Furthermore, these capsular entities also possessed an ionization event attributed to the deprotonation of a carboxylic acid with a shift of four pK_a units relative to free solution. We attributed this to the bound guest and the non-polar interior of the capsule greatly reducing its acidity. This deprotonation was found to de-cap smaller guest acids/carboxylates to form the corresponding 1:1 complex, but stearic acid/stearate **2b** was shown to always form the 2:1 host-guest complex irrespective of the pH of the external medium. In all cases discussed here, because of the high pH (~12) these guests exist predominately as their conjugate bases.

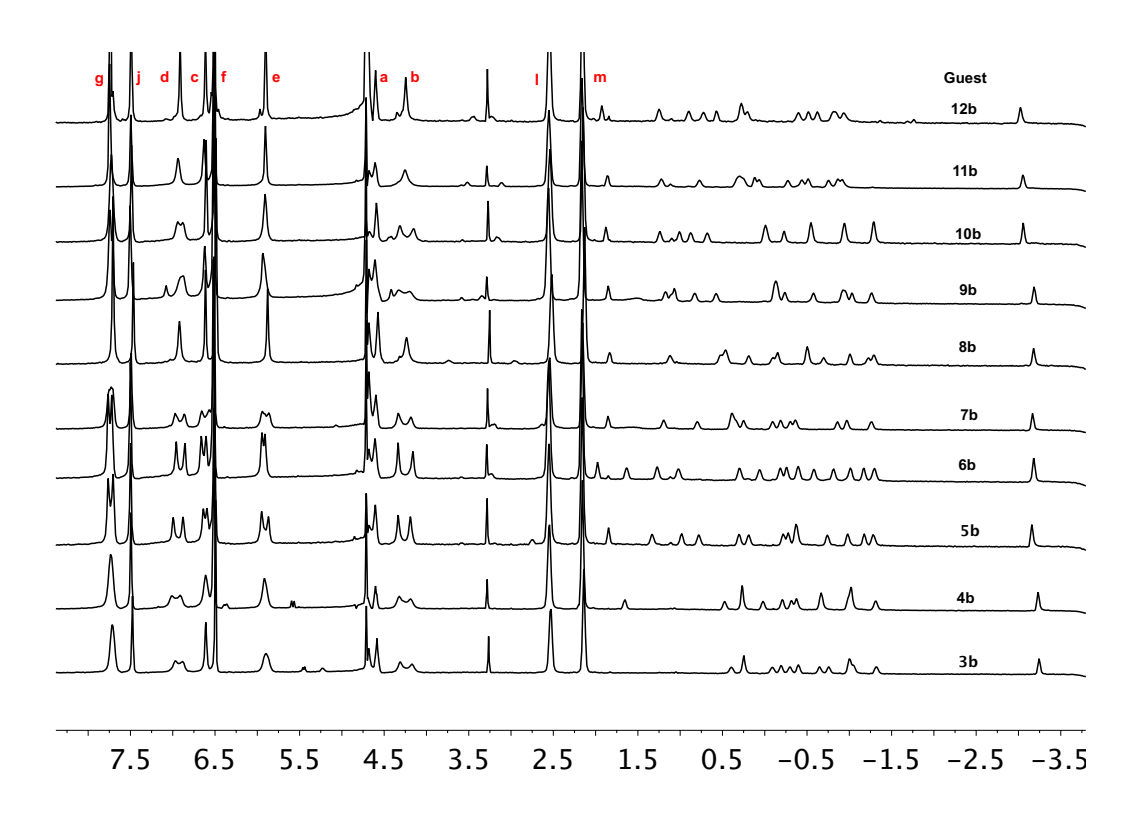


Figure 2: ¹H NMR spectra of encapsulated guest **3b-12b** within 1 mM host **1** in D₂O buffered with NaOD to pH ~12.

Figure 2 shows the ¹H NMR spectra for the resulting complexes with carboxylates **3b-12b** at a host-guest ratio of 2:1. DOSY NMR analysis confirmed that all these were 2:1 host guest complexes (Supporting Information). Each guest binding region in the spectra showed wide signal anisotropy, with an envelope of signals amounting to a distinct, unique signature for that complex. In all cases however, the position of the terminal C18 signal was remarkably consistent: –3.17 (± 0.14) ppm. Also evident from Figure 2 was splitting of the host signals in some of the complexes. For example the H_d signal (see structure **1**) at ~6.7 ppm is sharp in the case of **12b**, broad in the case of **9b**, and split into two singlets in the case of **6b**. The addition of a slight excess of guest revealed that in these complexes exchange between the free and the bound state is close to the NMR timescale, however this fact cannot account for the splitting of host signals such as in the case of the complex with **6b**. Consequently, this splitting of the host signals was attributed to relatively slow tumbling of the guest within the capsule (*vide infra*).

The upfield shifting of the bound guest signals relative to the free state arises because of the shielding properties of the aromatic walls of the container. It has been previously shown by both 1 H NMR, and molecular simulation and guest proton chemical shift evaluation using Gauge Invariant Atomic Orbital calculations, that in these types of capsular complexes, the deeper a guest atom is on average located in one of the hemispheres the greater the peak shift ($\Delta\delta$) between the free and the bound state. 22,49 To understand the packing motifs of these guests we therefore used COSY NMR to reveal the coupling between the bound guest signals, identify them, and calculate the corresponding $\Delta\delta$ value for each group (Supporting Information). Figure 3 shows the $\Delta\delta$ values for all of the methylene and methyl signals of guests **3b-12b**.

En masse this data landscape reveals ridges for methylenes C2-C3 and C12-C13 corresponding to limited upfield shifting of these signals, a valley centered on methylenes C7-C9 corresponding to strongly upfield shifted signals, and very large upfield shifts for the C18 terminus of each guest. Hence this data reveals that all carboxylates 3b-12b primarily adopt a J-shaped motif within 1_2 , with the terminal methyl group deeply buried at one pole forming strong C–H···· π interactions with the host, a turn at C7-C9 located at the other, and the carboxylate group at the equatorial region of the capsule (Figure 4). The near uniformity of the data landscape also shows that the location and stereochemistry of the bond has little effect on the preferred motif of a guest. We attribute this singular packing motif for all the guests to two factors. First, the solvation requirements of the polar carboxylate group; if this head group is located at the equatorial region of the host, small-scale opening of the capsule (its breathing), for all low partial solvation. The packing of these carboxylates and the corresponding esters

(*vide infra*) therefore reveal the first evidence of heterogeneity in the polarity of the inner space of the container **1**₂. To our knowledge this type of guest anchoring has not been identified in other, all-encapsulating supramolecular hosts. Second, the sharpness of the methyl group, the flexibility of its attendant chain, and the overall low polarity of these moieties make the alkyl chain an efficient packer of the non-polar and relatively narrow polar region of the capsule.²² In combination, these factors dominate packing and ensure a singular type of binding. It is illustrative to compare this J-shaped motif with comparably long alkane guests such as *n*-octadecane, *n*-nonadecane and *n*-eicosane, which due to symmetry reasons adopt U-shaped motifs.²²

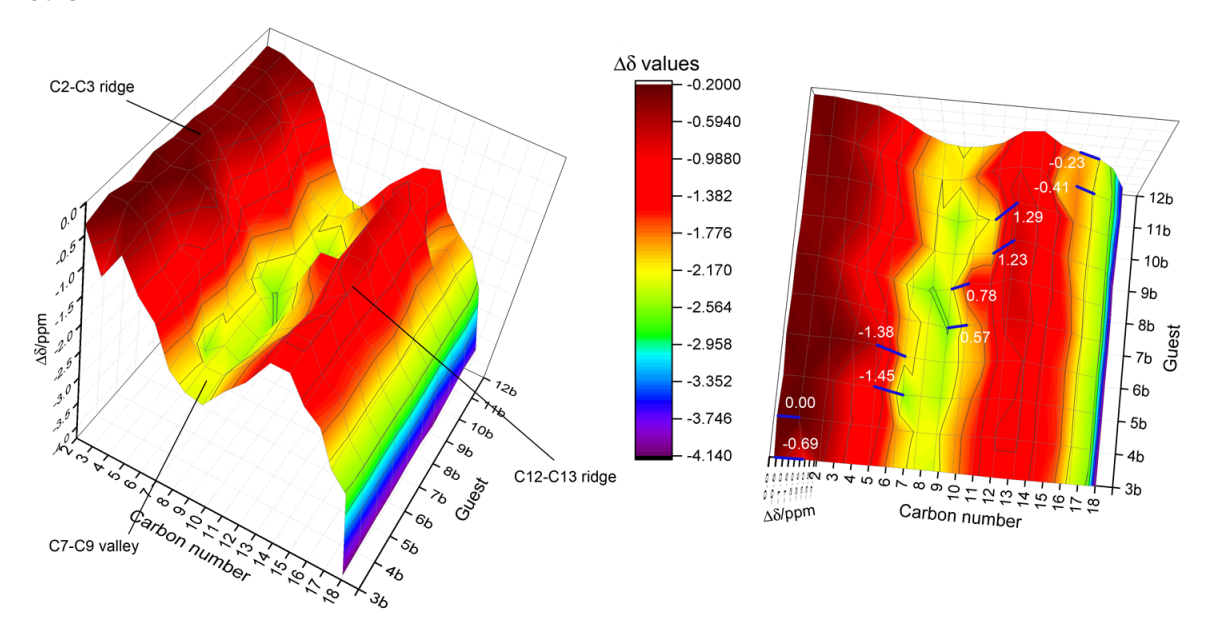


Figure 3: 3D plot of $\Delta\delta$ values for groups C2-C18 of encapsulated guest **3b-12b**. Left. Perspective highlighting: 1) C2-C3 and C12-C13 ridges, the C7-C9 valley corresponding to the turn of the J-motif, and the extreme upfield shifts for the C18 termini. Right. Plan perspective looking down on the same $\Delta\delta$ landscape for encapsulated guest **3b-12b**. The location of the double bonds in the different guests is highlighted using blue lines. Indicated values are the $\Delta\Delta\delta$ for the alkene methine signals (see main discussion).

Looking at the $\Delta\delta$ landscape more closely, Figure 3 also shows (right) the corresponding plan perspective, with the position of the double bonds in each isomer indicated as a blue line. Assuming that the maximal $\Delta\delta$ values in the midsection of the guest corresponds to the position of the turn, its precise position is slightly different for each guest; in general for guests **3b-6b** the double bond is located on the shorter (carboxylate-terminated) arm of the J-motif, whilst for guests **7b-12b** the double bond is located in the longer (methyl terminated) arm of the motif (Figure 4). In the case of *cis*-6 **5b** and *trans*-9 **8b** (elaidic acid) the reverse turn is relatively early in the chain (Figure 3 right). We interpret these findings to the *cis*-6 double bond of **5b**

being more predisposed for the turn and promoting the early reversal of direction, whilst the incongruity of a *trans*-9 double bond in **8b** for the narrow polar region of the capsule does likewise. Between these two isomers is *cis*-9 **7b** (oleic acid) where the ideal geometry of the double bond results in it being part of the turn. The C7-C9 turn of *trans*-15 guest **11b** also stands out from the average. Thus although the double bond is well removed from the turn, the upfield shifting of the turn is relatively small. This suggests that on average the turn is not deeply located in one polar region of the capsule.

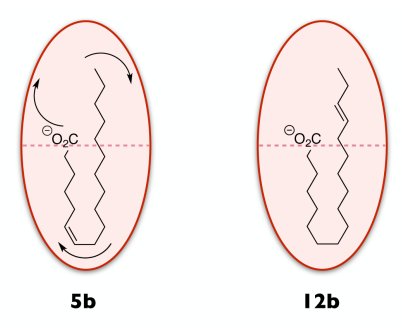


Figure 4: Schematic representations of the complexes involving guests **5b** and **12b** as representative examples of the J-shaped packing motif of acid guests **3b-12b**.

The labels for each blue line indicating the position of the double bond in Figure 3 are the attendant $\Delta\Delta\delta$ values for the alkene methine signals, i.e., the difference in the extent that each vinylic proton is shifted upfield when in the bound state. As the alkene group has limited flexibility and its methines possess very similar chemical shifts in the free state, a comparison of the magnetic environment of the two signals in each guest gives a report of the heterogeneity of the electronic environment around the double bond. For example, in the case of **12b** these two protons are in very similar electronic environments ($\Delta\Delta\delta$ = 0.23 ppm), whereas the corresponding methine groups of guest **5b** reside on average in very different surroundings ($\Delta\Delta\delta$ = 1.45 ppm). In this latter case the C7 is bound near the very base of the pocket whereas the adjacent C6 methine is located above it (Figure 4). It is interesting to consider the possibility that these different magnetic environments may indicate the possibility of controlling the regioselectivity of addition reactions to such guests.

The J-shaped motif for these guests represents a time-average sum of the different conformations weighed according to their relative energies. Thus, in the case of **6b** the desymmetrization of the host capsule (e.g., H_d, Figure 2) arises because the tumbling of the guest (Figure 4 left) is slow on the NMR time-scale. However, this tumbling is evidently close to the NMR timescale; the complex with **9b** has very broad host signals, whereas binding **12b**

results in an apparently symmetric capsule. To confirm this hypothesis a VT 1 H NMR experiment was carried out with guest **6b** (Figure 5). At room temperature, the H_c and H_d signals are split into two singlets, but as the temperature was raised these signals coalesced and ultimately at 70 $^{\circ}$ C each appear as a sharp singlet.

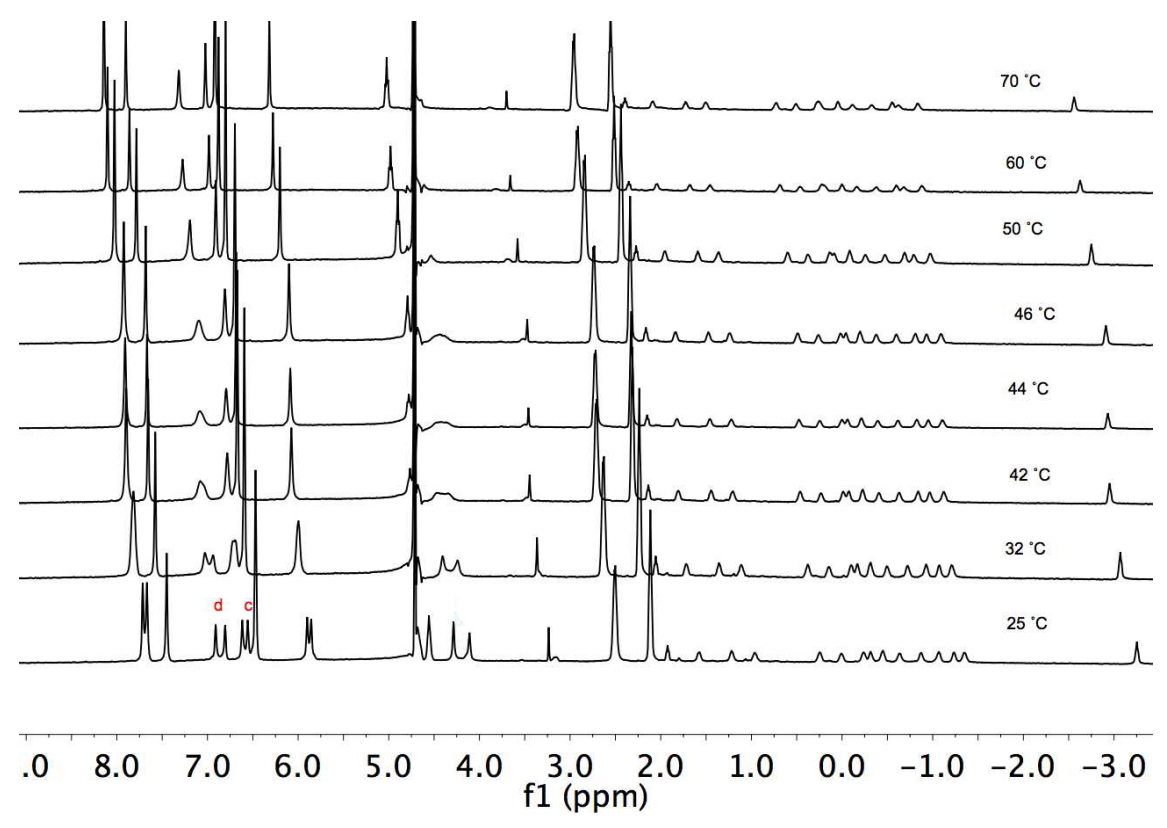


Figure 5: VT ¹H NMR spectra of encapsulated guest **6b** within 1 mM host **1** in 100 mM NaOH/D₂O.

To ascertain how the position and stereochemistry of the double bond affects the coalescence temperature (T_{coal}) we carried out VT NMR studies of all of the complexes of carboxylates **3b-12b**. This revealed an order of increasing T_{coal} values for this series of guests as (°C): **12b** (10), **8b** (12), **11b** (14), **3b** = **4b** (30), **9b** (31), **7b** = **10b** (34), **5b** (41), **6b** (44). Thus although the location of the double bond in these guests is not reflected in significant changes in their packing motif, the kinetics of tumbling is more significantly affected (Figure 6). The guests can be roughly grouped into two families. The kinetically most stable motifs consist of either *cis* double bonds located at the center of the main chain near the reverse turn (e.g., **5b**), or *trans* double bonds located away from the turn and in the arms of the J-shaped motif (e.g. **10b**). The other guests have much lower T_{coal} values. These include those with double bonds near the termini (**11b**, and **12b**) or a *trans*-9 double bond (**8b**) near the turn in the molecule. As

Figure 3 shows, guests **11b**, and **12b** have relatively small upfield-shifted reverse turns at C8-C9 indicative of a far from ideal packing of the polar region by the reverse turn. Precisely how the packing of **11b** and **12b** differs from the others is not clear from this data, but evidently their preferred motif is relatively high in energy and the resulting T_{coal} values much lower. One possibility is that the attenuated upfield shift of their turns and low T_{coal} values are a reflection of the difficulties with storing a relatively rigid C15-C18 moiety in the narrowest polar region of the capsule. In contrast, the low T_{coal} for the complex with **8b** seems evident; the situation of having a *trans* double bond near to the reverse turn of the bound guest is far from ideal.

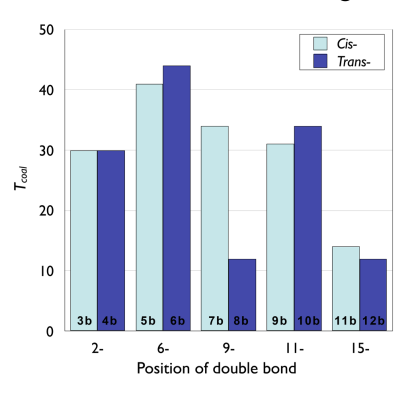


Figure 6: Influence on the position/stereochemistry of the double bond upon T_{coal} for the carboxylate guests **3b-12b**.

In summary, the position and the stereochemistry of the C=C double bond in carboxylates **3b-12b** do not influence the gross overall conformation or motif of the different guests; the J-shaped motif is controlled by the anchoring effect of the terminal methyl group and the carboxylate binding to the polar and equatorial regions of the capsule respectively. However, there are subtle differences between the motifs of the guests, and the position and stereochemistry of the double bond do influence the movement of the guest within the capsule.

Methyl esters 2a-12a binding to octa-acid 1

To investigate the binding motifs of the fatty acid methyl esters inside the capsule formed by octa-acid ($\mathbf{1}_2$), we performed the same suite of analytical techniques utilized for studying the carboxylate complexes. Namely ¹H NMR was used to confirm a 2:1 host-guest stoichiometry, DOSY NMR was used to confirm a dimeric capsule structure, whilst a combination of COSY and NOESY NMR experiments allowed guest peak assignment and revealed the $\Delta\delta$ values for the bound guest signals. Figure 7 shows the $\Delta\delta$ values for all of the main-chain methylene and methyl signals of guests **3a-12a**, and reveals a more complex $\Delta\delta$ landscape than that seen for the carboxylate complexes (Figure 3).

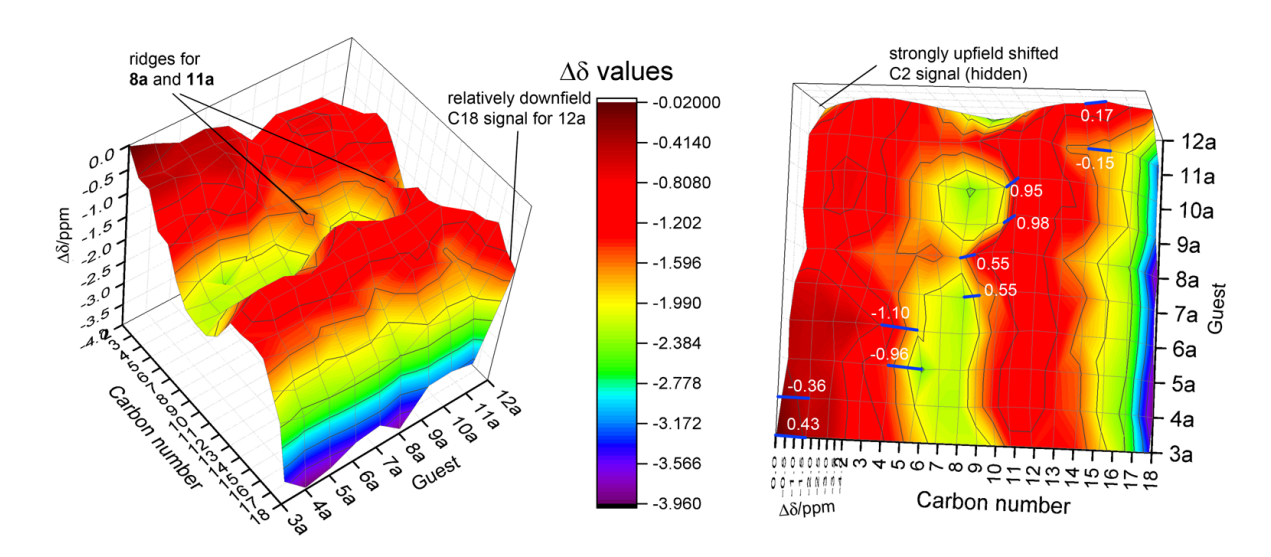


Figure 7: 3D plot $\Delta\delta$ values for groups C2-C18 of encapsulated guest **3a-12a**. Left. Perspective highlighting: 1) the strong, but variable upfield shifts for the C18 methyl, and in particular the small shift in the C18 methyl signal for **12a**. Also highlighted are saddles for guests **8a** and **11a** that cut across the C7-C9 valley. Right. Plan perspective looking down on the same $\Delta\delta$ landscape for encapsulated guest **3a-12a**. The location of the double bonds in the different guests is highlighted using blue lines. Indicated values are the $\Delta\Delta\delta$ for the alkene methine signals.

There are several key, gross topological differences between the $\Delta\delta$ landscapes of these two sets of guests. In particular, the major ridges at C2-C3 and C12-C13 for esters 3a-12a are generally more varied than the corresponding carboxylates. For example, the upfield shifting of the C2 signal varies from -0.02 to -1.93 ppm for the esters (3a and 12a respectively), whereas the same signals from the carboxylate guests range from -0.21 to -0.39 ppm (for 4b and **9b** respectively). Relatedly, the $\Delta\delta$ values for the terminal C18 signal for the esters vary from -1.38 ppm in the case of 12a to -3.95 ppm in the case of 4a, whereas the C18 signals for the bound carboxylates were spread over a narrow range from -3.76 to -4.14 ppm (11b and 3b respectively). Equally as significant, the C7-C9 valley of the ester guest $\Delta\delta$ landscape is punctuated by two saddles corresponding to minimally upfield-shifted turns for guests 8a, 11a Evidently, the decreased polarity of the ester group relative to the carboxylate and **12a**. reduces the influence that this terminus has on guest packing and hence allows for more variety in the different possible guest motifs. Analysis of the series of complexes reveals three different motifs exemplified by guests 5a, 8a, 11a and 12a. The ¹H NMR spectra of these complexes are shown in Figure 8.

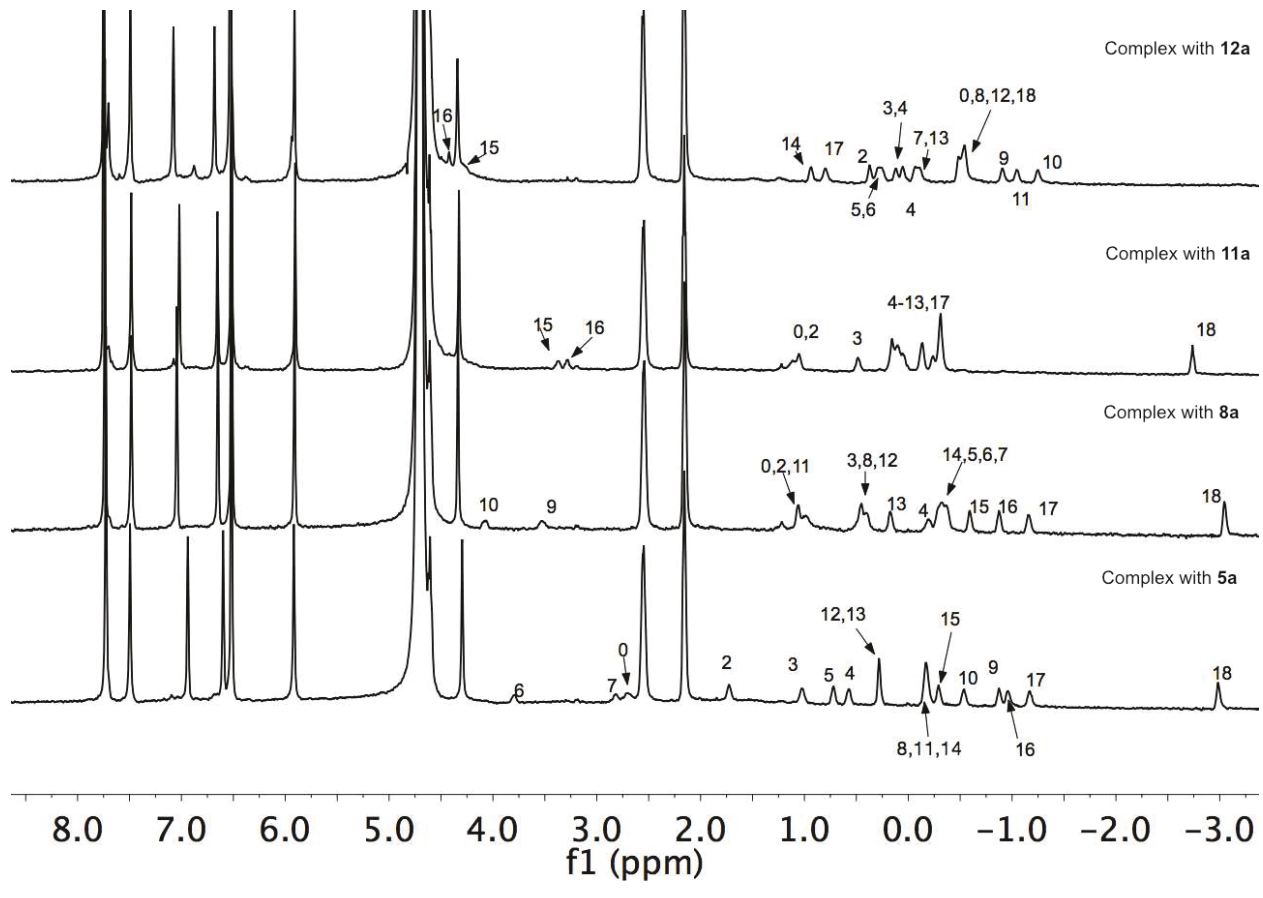


Figure 8: ¹H NMR spectra of encapsulated guests **5a**, **8a**, **11a and 12a** within 1 mM host **1** in 10 mM Na₂B₄O₇/D₂O. Bound guest signals are labeled as per Figure 1.

The complex formed by cis-6 isomer **5a** is typical of a J-shaped guest binding-motif analogous to the carboxylate guests. Of all the moieties in this guest it is the C-18 terminal methyl that was shifted upfield to the greatest extent ($\Delta\delta$ = -3.82 ppm). The reverse turn in bound **5a** was indicated by the significant upfield shifts of the C7, C8 and C9 methylene groups signals which possess $\Delta\delta$ values of -2.42, -2.15 and -2.22 ppm respectively. In contrast, the C2 and methoxy (C0) groups were shifted upfield only by respectively -0.46 and -0.79 ppm. Additionally, the alkene methine signals of **5a** possessed a relatively large $\Delta\Delta\delta$ value (the difference between how much each methine is shifted upfield when moved from the free to the bound state) indicating that on average each methine resides in quite different electronic environments (Figure 7). Thus in combination these NMR shifts results demonstrate that **5a** adopts a J-shaped motif in which the cis-6 double bond is located on the short (ester terminated) arm and at the turn of the motif (Figure 9).

The guest binding region of the complex with *trans*-9 guest **8a** shows the largest signal anisotropy with a spread of over 7 ppm (Figure 7 and 8). Nevertheless, at room temperature

many of the guest signals were broad and overlapping. To fully characterize the signals from this guest a VT NMR experiment was performed which gave improved signal resolution at 50 °C (Supporting Information). Integration of the peaks at this elevated temperature, combined with a COSY NMR experiment, led to the assignment shown in Figures 7 and 8. In this particular case the uncoupled methoxy group signal overlapped with those from C2 and C11 and did not apparently integrate for three protons. Extended delay times in the NMR experiment did not resolve this issue, so we sought to confirm this assignment using ²H NMR. corresponding deuterated methyl ester was synthesized by treating 8b with HCl in d4-MeOH and the deuterium NMR of its corresponding complex recorded in H₂O (Supporting Information). The lower resolution of ²H NMR and the restricted movement of the quest was evident in the broadness of the CD₃- signal, but accounting for the isotope effect on chemical shift these experiments confirmed the location of the methoxy signal in the ¹H NMR spectrum of the complex. Thus, the methoxy (C0) and the C2 signals, as well as the C18 signal, were considerably upfield shifted: $\Delta\delta$ = -2.32, -1.21 and -3.96 ppm respectively. In contrast to the Jshaped guest 5a, the most upfield shifted methylene in the midsection of 8a, C9, was only shifted by -1.79 ppm. This smaller shift in the signals from the midsection of 8a, coupled with the much larger shift in the signal from the methoxy (C0) group, suggests that rather than adopting primarily a J-shaped motif, the trans-9 double bond of guest 8a shifts the preferred motif to one that is more U-shaped. In other words there is little energetic preference as to which of the termini binds to the polar region. NOESY NMR of the complex supports this idea with cross peaks between the C-2 and C3 methylene signals and the H_b signals from the host (Supporting Information). As with the carboxylate guest 8b, the trans-9 double bond of 8a is located after the turn in the guest, and the small difference between its two methine signal shifts indicates that both carbons are at similar depths in the pocket. We interpret these findings to the poor fit of the trans double bond in the turn and at the narrow, polar region of the capsule. This misfit prevents the turn fully occupying the base of the host, leads to relatively small upfield shifting of the signals at this point in the guest, and forces the ester group more deeply into the opposing pole of the capsule (Figure 9, c.f. 6a). These factors were also evident in the complex of 8b, but are not so pronounced because of the stronger anchoring properties of the carboxylate for the equatorial region of the capsule. In other words when the carboxylate head group is replaced by the methyl ester the reduced polarity of the group allows the guest to readjust to a U-shaped motif to relieve the misfit of the double bond.

Considerable clustering of signals was evident in the ¹H NMR spectrum of the complex with **11a** (Figure 8). Moreover, the overall anisotropy for the bound guest signals was relatively

low, covering a range of 6.00 ppm. The overlap of signals was improved at 40 °C (Supporting Information), and this allowed complete assignment of the guest signals (Figure 7) and the determination of the packing motif inside the capsule formed by 1. The C-18 terminal signal was the most upfield shifted, but only to a relatively small extent ($\Delta \delta = -3.76$ ppm). Likewise, compared to other guests the midsection of 11a also underwent the least upfield shifting, by only $\Delta \delta = -1.40$ ppm in the case of C8. Finally, much like 8a, the methoxy (C0) and C2 signals of 11a were also shifted considerably upfield, by $\Delta \delta = 2.20$ and -1.01 ppm respectively. This is again consistent with a U-shaped binding motif. A re-examination of the $\Delta \delta$ landscape for the complex with carboxylate 11b (Figures 3) highlights a spur that rises in the C7-C9 valley that, in the case of 11a, is exacerbated to the point of forming a saddle between the two main ridges. Moreover, 11b possessed one of the lowest recorded T_{coal} values of the carboxylate guests. These results therefore highlight that a *cis*-double bond is not well accommodated near the terminus of the long chain of the guest, presumably because it is too inflexible to efficiently fill the narrow polar region of the capsule. Consequently, a reduction of the polarity of the head group by methylation allows guest 11a to adopt a more relaxed U-motif.

The NMR spectrum for the complex with guest 12a (Figure 8) is instantly distinctive with its lack of highfield methyl signal; the absence of this signal leads to the narrowest anisotropy for the series, ~5 ppm. Full characterization of the bound guest signals revealed that the terminal C18 and the methoxy (C0) group had $\Delta\delta$ values of -1.38 and -4.21 ppm respectively; uniquely, the methoxy (C0) is considerably more upfield shifted than the C18 terminus. Correspondingly, the C2 methylene signal shifted upfield an exceptional -1.93 ppm. In contrast, the midsection of the guest (C10) was shifted a typically large amount: $\Delta\delta$ = -2.49 ppm. These observations are consistent with a reverse J-shaped binding motif whereby the ester group is located deep in one of the poles of the capsule, and the terminal methyl group is located near the equator (Figure 9). NOESY NMR confirmed this (Supporting Information), with the only evident through-space interactions between the guest and the H_b protons of the host involving the methoxy (C0) and the C9-C11 methylenes. We attribute this change in binding motif to the inflexibility and narrower profile of the *trans*-butene terminal group making it an even poorer packer of the narrow, polar region of the capsule than the terminus of its *cis*-counterpart 11a.

Figure 9 shows a summary of the different binding motifs for each guest **3a-12a**. Most of the guests adopt J-motifs in which the ester group is located near to the equator of the capsule. However within this group of seven guests, **9a** and **10a** possess relatively large $\Delta\delta$ values for the C2 methylene and relatively small $\Delta\delta$ values for the C18 groups. This suggests that their preferred motif is somewhat between a J-shape and a U-shape, but we classify them as the

former owing to the relatively large difference between the $\Delta\delta$ values of the two termini.

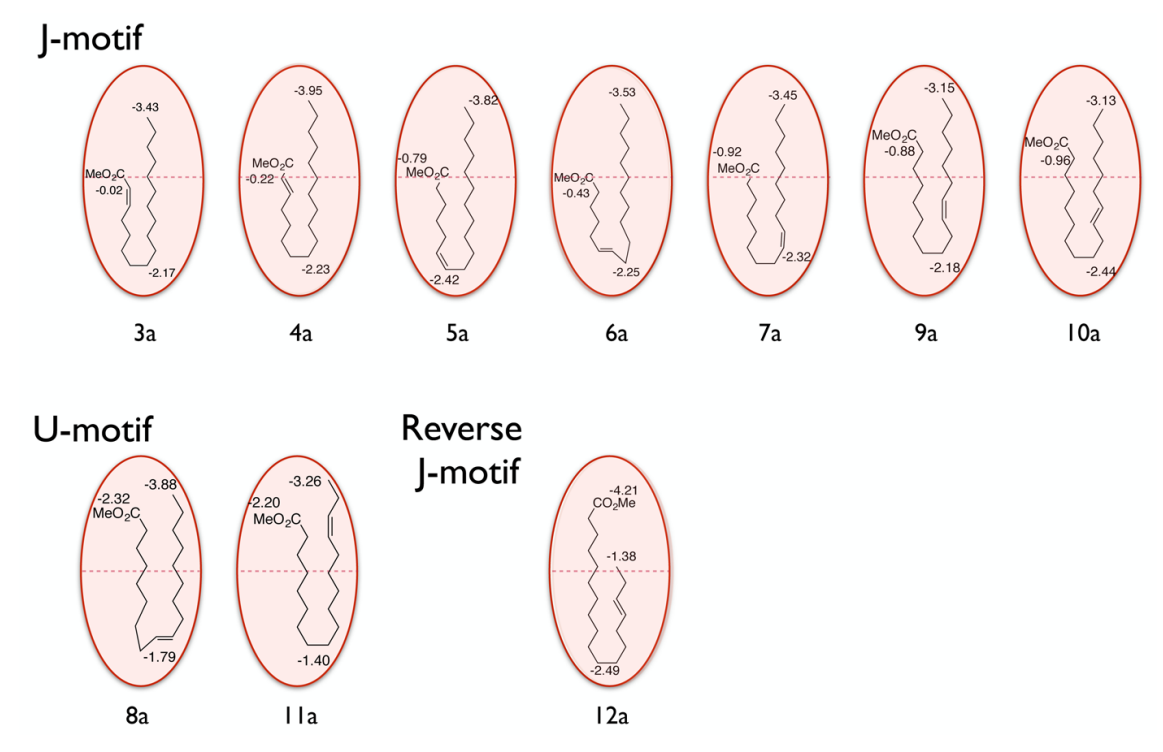


Figure 9: Summary of approximate packing motifs of guests 3a-12a. Shown numerals are the $\Delta\delta$ values for the methoxy (C0), C2 (if the methoxy signal was not observed) and C18.

Comparisons between the different complexes reveal the importance of the position and the stereochemistry of the singular double bond in this guest family. For example there is little motif change between stereoisomers **3a** and **4a**, **5a** and **6a**, or between **9a** and **10a**. However, there are motif switches between **7a** and **8a**, and between **11a** and **12a**. On the other hand, within the *cis* isomers there are four J- and one U-motif, whilst within the *trans* isomers there are three J-, one U-, and one reverse J-motif.

Having determined the binding motif of each guest within the dimer formed by octa-acid 1, we performed a cross-checked network of paired competition experiments to determine the relative binding constants for the five pairs of guests (Supporting Information). For these determinations either integration of the bound H_c or H_d peak from the host or the bound guest methyl peaks could be utilized. By this approach the relative binding constants for the guests were found to increase in the series (K_{rel}): 3a (1), 12a (3), 4a (5), 11a (10), 8a (17), 10a (20), 6a (27), 9a (41), 5a (56) and 7a (67). Figure 10 plots this data as a function of the position and stereochemistry of the double bond. For all but one stereoisomeric pair, the cis isomers have stronger binding affinities with 1_2 than the trans isomer. We ascribed this observation to the

overall more compact shape of the *cis*-isomers conforming to the confining space of the capsule. In addition, Figure 10 demonstrates that the closer a double bond is to one of the termini, the weaker the complex. Evidently, restricted conformations for groups that must reside at the narrower polar regions of the capsule weakens affinity. Another way of stating these two observations is that the most stable complexes are formed by *cis*-mono-unsaturated esters where the double bond is ideally placed for promoting the turn in the J-shaped binding motif, e.g., in the *cis*-6, *cis*-9 and *cis*-11 guests **5a**, **7a** and **9a**. Interestingly, within experimental error these bind as strongly or more strongly than the corresponding saturated ester **2a** ($K_{rel} = 42$).

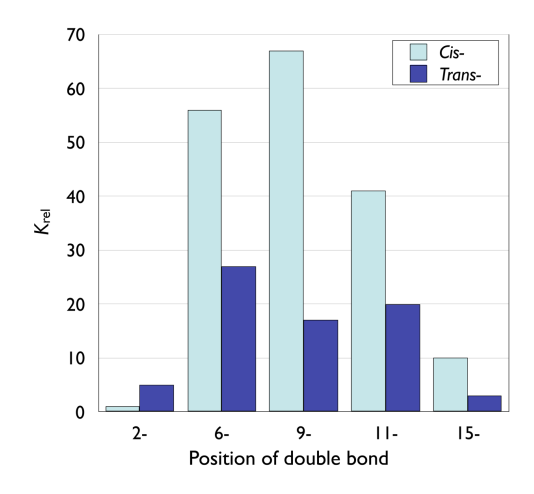


Figure 10: K_{rel} values: as a function of the position and stereochemistry of the double bond in guests 3a-12a.

Although the double bond strongly influences the relative affinity of the guests, we were not able to confirm that its position or stereochemistry affect the T_{coal} of the guest. Thus, of all the esters examined only the complex with *trans*-2 **4a** showed any signs of broadening of the H_c and H_d signals at room temperature (Supporting Information). We carried out a VT NMR study on this complex and ascertained that its T_{coal} was 12 °C. Hence the esters clearly tumble much more rapidly within the capsule than the considerably more polar carboxylate guests – a reflection of the weaker anchoring effect of the ester groups – and only with the *trans*-2 double bond of **4a** can this motion be inhibited such that desymmetrization of the capsule is apparent.

Conclusions

Our previous studies with relatively small constitutionally isomeric, unbranched esters $(C_{11}H_{22}O_2)$ revealed a straightforward pole-to-pole binding motif for all guests.¹⁵ However, the C18 guests studied here reveal a much more complex picture with larger guests. The binding motif of the carboxylate guests is dominated by the propensity for the terminal methyl group to anchor to the narrow walls of the poles of the capsule via $C-H\cdots\pi$ interactions, and for the

carboxylate group to be anchored at the equatorial region of the host. To our knowledge, this latter concept of guest anchoring because continual breathing of the capsule leads to a more polar environment around the equatorial region of the host is unique to encapsulating supramolecular hosts. The result of this twin anchoring is a near uniform J-shaped motif for guests 3b-12b. However, the position and stereochemistry of the double bond does have a significant impact on the kinetics of guest movement within the capsule. In contrast, when the polarity of the head group is diminished by methylation, this equatorial anchoring by the head group is attenuated. As a result the methyl esters were found to bind in three different binding motifs; depending on the position and stereochemistry of the C=C double bond, the guests were found to adopt either a J-shaped, U-shaped or a reverse J-shaped motif. The fact that the Jshaped motif also predominates suggests that although ester groups are weaker equatorial anchors than carboxylates, in most cases the alkyl chain is a better packer of the polar regions of the capsule than the ester moiety. The exceptions to this are when the sole C=C double bond is near the terminus of the main-chain, in which case the reduced flexibility of the tail of the main-chain reduces its ability to pack the polar regions of the capsule relative to the ester group. In that regard the trans double bond geometry of 12a is the poorest packer of the guests examined here, and a reverse J- shaped motif of this guest is preferred. A double bond highly incongruous with the reverse turn of the bound guest – the trans double bond of 8a – also shifts the packing motif away from the typical J-shaped motif, in this instance to a U-shaped motif.

The lower polarity of the ester guests relative to the carboxylates result in the former being more mobile within the container, but this lower polarity also leads to slow exchange between the free and the bound state. This latter fact allowed the relative binding constants (K_{rel}) of the ester guests to be determined, and revealed that the affinity for the capsule was highly dependent on the position and stereochemistry of the double bond. At the most general level, guests with cis-double bonds in the middle of the main-chain possess the highest affinity, whilst unsaturation near one of the termini of the guest lead to lower stabilities.

To our knowledge, these results represent an unprecedented level of guest motif mapping, and demonstrate how such mapping can identify heterogeneities with the inner space of molecular and supramolecular containers. These results also demonstrate the potential for yocto-liter containers to bring about exquisitely selective reactions upon bound guests. On that topic, on the expectation that these varied binding motifs considerably affect the rates of hydrolysis of encapsulated esters **3a-12a**, we are currently investigating kinetic resolutions using these complexes. These results will be reported in due course.

Experimental Section

1) Materials and Instrumentation

Host **1** was synthesized following the previously reported procedure.^{37,38} All NMR spectra were recorded on a Bruker 500 MHz spectrometer at 25 °C unless otherwise stated. Spectral processing was carried out using Mnova software (Mestrelab Research S.L). All reagents and guests **2a**, and **5a-10a** (Figure 1) were purchased from Aldrich and were used without purification. The remaining (known) guests **3a**, **4a**, **11a** and **12a** were synthesized by using Wittig chemistry. Known acid guests **2b-12b** were generated as complexes *in situ* by adding NaOH solution to the corresponding ester guest complexes.

2) Synthesis of guests 3a and 4a

The synthesis of guests **3a** and **4a** (Scheme 1) followed procedures described previously.⁵¹

Synthesis of hexadecyltriphenylphosphonium bromide

1-bromohexadecane (10 mmol, 3.05 g) and triphenylphosphine (5 mmol, 1.30 g) was added to toluene (40 mL) and the solution was heated to 90 °C. After two days, the reaction was cooled and concentrated under reduced pressure to afford the crude phosphonium salt that was washed with 50 mL diethyl ether. 2.2 g (79% yield) of precipitated phosphonium salts were collected and dried under vacuum. ³¹P NMR (162 MHz, Chloroform-d, ppm): δ = 25.66 (s, R-PPh₃⁺, ref. = -4.42 (s, PPh₃).

Synthesis of guests 3a and 4a

To a suspension of hexadecyltriphenylphosphonium bromide (7.0 mmol, 4.0 g) in anhydrous THF (10 mL) at 0 °C under nitrogen was added NaN(TMS)₂ (1.0 M in THF, 6.43 mmol). The resulting orange mixture was stirred for 40 min. at rt. Methyl 2-oxoacetate (3.5 mmol 300 mg) in THF (5 mL) was then added drop-wise by syringe. After 3 h. the reaction was quenched with saturated aqueous NH₄Cl (20 mL), and extracted with DCM (3 × 50 mL). The combined extracts were dried over anhydrous Na₂SO₄, and DCM was removed under reduced pressure. The residue was purified on silica gel by stepwise gradient elution with dichloromethane/hexane (20:80 to 50:50). Guests **3a** and **4a** were isolated in a 60:40 ratio (500 mg, 48% and 331 mg, 32% respectively). **3a**: 1H NMR (500 MHz, Chloroform-d, ppm): δ 6.25 (dt, J = 11.5, 7.5 Hz, 1H), 5.79 (d, J = 11.5, 1H), 3.73 (s, 3H), 2.67 (m, 2H), 1.46 (p, J = 7.3 Hz, 2H), 1.28 (m, 24H), 0.91 (t, J = 6.9 Hz, 3H). **4a**: 1H NMR (500 MHz, Chloroform-d, ppm): δ 7.05

-6.95 (dt, J = 15.7, 7.0 Hz, 1H), 5.84 (d, J = 15.7 Hz, 1H), 3.75 (s, 3H), 2.22 (m, 2H), 1.47 (p, J = 7.1 Hz, 2H), 1.29 (m, 24H), 0.91 (t, J = 6.9 Hz, 3H).

3) Synthesis of guests 11a and 12a

Guests **11a** and **12a** were synthesized (Scheme 2) by a similar procedure to that outlined by Rawling *et al.*,⁴⁷ and were distinguished using FT-IR and ¹³C NMR. Thus, as has been previously reported,⁵² guest **12a** showed an absorbed band at 967 cm⁻¹, whereas for **11a** this band was absent but an absorption at 3001 cm⁻¹ was evident. Again consistent with previous a report,⁵³ in the ¹³C NMR spectrum the allylic carbons resonances of **11a** were evident at 27.10 ppm (C14) and 20.51 ppm (C17)m while those of **12a** were observed at 32.59 ppm and 25.60 ppm.

Synthesis of methyl 15-hydroxypentadecanoate

To a solution of the hydroxy fatty acid (7.00 mmol) in acetone (120 mL) was added water (8 mL), potassium carbonate (20.00 mmol) and iodomethane (35.00 mmol). The resulting mixture was refluxed for 4 h, and then concentrated under reduced pressure. The residue was dissolved in water (60 mL), and the solution was acidified with 1 M HCl. The aqueous phase was extracted with DCM (3 × 60 mL), and the combined extracts were washed with brine (100 mL), dried over Na₂SO₄, and concentrated under reduced pressure to afford 1.80 g of the methyl ester (95% yield). 1 H NMR (400 MHz, Chloroform-d): δ 3.64 (s, 3H), 3.61 (m, 2H), 2.28 (t, J = 7.6 Hz, 2H), 1.59 (m, 2H), 1.24-1.33 (m, 22H).

Synthesis of Methyl 15-oxopentadecanoate

Under nitrogen, methyl 15-hydroxypentadecanoate (4.00 mmol) in anhydrous DCM (6 mL) was added to a suspension of pyridinium chlorochromate (PCC, 6.68 mmol) and Celite (1.440 g) in 20 mL of anhydrous DCM. The mixture was stirred for 2 h., after which time diethyl ether (50 mL) was slowly added. The resulting mixture was stirred for 10 min, and then filtered over Celite. The Celite was washed with ether (2 × 20 mL), and the filtrate concentrated under reduced pressure. The residue was purified on silica gel by stepwise gradient elution with dichloromethane/hexane (40:60 to 100:0) to give 0.90 g of the aldehyde (84% yield). ¹H NMR (500 MHz, Chloroform-d): δ 9.79 (t, J = 1.9 Hz, 1H), 3.69 (s, 3H), 2.43 (td, J = 7.3 Hz, 1.9 Hz, 2H), 2.32 (t, J = 7.5 Hz, 2H), 1.56 (m, 4H), 1.40 – 1.24 (m, 18H).

Synthesis of guest 11a

Under nitrogen, NaN(TMS)₂ (1.0 M in THF, 6.43 mmol) was added to a suspension of n-propyltriphenylphosphonium bromide (7.00 mmol) in 10 mL anhydrous THF at 0 °C. The resulting orange mixture was stirred for 1h at rt. The solution was then cooled to -78 °C, and methyl 15-oxopentadecanoate (3.21 mmol) in 5 mL anhydrous THF was added dropwise by syringe. The mixture was stirred at -78 °C for 30 min after which time the reaction mixture was allowed to warm to rt. After further stirring for 2 h the reaction was quenched with 20 mL saturated aqueous NH₄Cl and extracted with DCM (3 × 50 mL). The combined extracts were dried over anhydrous Na₂SO₄, and the solvent removed under reduced pressure. The residue was purified on silica gel by stepwise gradient elution with dichloromethane/hexane (20:80 to 50:50) to give 690 mg of **11a** (75% yield). ¹H NMR (500 MHz, Chloroform-d, ppm): δ 5.37 (m, 2H), 3.69 (s, 3H), 2.33 (t, J = 7.6 Hz, 2H), 2.06 (m, 4H), 1.65 (p, J = 7.3 Hz, 2H), 1.30 (m, 18H), 0.98 (t, J = 7.5 Hz, 3H).

Synthesis of guest 12a

To a solution of *cis*-15 ester **11a** (100 mg, 0.34 mmol) in DCM, was slowly added *m*-CPBA (70 mg, 0.41 mmol). The mixture was further stirred for 2 h at rt. Excess *m*-CPBA was subsequently destroyed by the addition of a solution of sodium sulfide (20 mL). The DCM was then removed to give the crude epoxide (95 mg, 90% yield). To a rt solution of this epoxide (0.005 mol) in 15 mL anhydrous THF under nitrogen was added lithium diphenylphosphide in anhydrous THF (4.15 mL, 1.15 M in phosphide). The resulting solution was allowed to stand until the red color of phosphide disappeared. Purified methyl iodide (1.5 equiv.) was then added and the mixture stirred for 20 min. at rt. After aqueous work-up, the organic phase was concentrated and analyzed by GC-MS. The residue was purified on silica gel by stepwise gradient elution with dichloromethane/hexane (20:80 to 50:50) to give 50 mg of **12a** (35% yield). ¹H NMR (500 MHz, Chloroform-d, ppm): δ 5.41 (m, 2H), 3.69 (s, 3H), 2.32 (t, J = 7.6 Hz, 2H), 2.06 (m, 4H), 1.65 (p, J = 7.2 Hz, 2H), 1.30 (m, 18H), 0.96 (t, J = 7.4 Hz, 3H).

3) Synthesis of acids 2b-12b

All acids were synthesized as their complexes with host **1** by the addition of excess NaOH (100 equiv.) to the capsular complexes of their respective ester.

4) General procedures of sample preparation for NMR studies

Unless otherwise noted, each experiment was carried out using a 600 μ L sample of 1.0 mM host 1 in 10 mM Na₂B₄O₇/D₂O buffer at 25 °C. To form the host-guest complexes the guests were first dissolved in acetone- d_6 to give a 30 mM stock solution. Subsequently, 10 μ L of each guest solution was added to the vial and the acetone removed with a stream of nitrogen. The vial was then dried at rt under reduced pressure for 5 min. The host solution was then added to the vial and the resulting solution stirred for 30 min. to give the corresponding 2:1 host-guest complex.

For all COSY and NOESY NMR experiments, a 10 μ L volume of 150 mM stock solution of guest in acetone- d_6 was combined with a 600 μ L volume of a 5 mM host solution in 50 mM Na₂B₄O₇/D₂O buffer.

Acknowledgements

The authors gratefully acknowledge the National Science Foundation (CHE-1507344) for financial assistance, and Matthew B Hillyer and J. Wes Barnett for technical assistance.

Supporting Information. Materials and instrumentation information, and details of NMR studies including $\Delta\delta$ value calculations for encapsulated guests, diffusion coefficient data, and coalescence temperature measurements.

References

- (1) Kang, J.; Rebek, J., Jr. Nature 1997, 385, 50-52.
- (2) Yoshizawa, M.; Tamura, M.; Fujita, M. Science 2006, 312, 251-254.
- (3) Pluth, M. D.; Bergman, R. G.; Raymond, K. N. Science 2007, 316, 85-88.
- (4) Nishioka, Y.; Yamaguchi, T.; Yoshizawa, M.; Fujita, M. *J. Am. Chem. Soc.* **2007**, *129*, 7000-7001.
- (5) Kaphan, D. M.; Levin, M. D.; Bergman, R. G.; Raymond, K. N.; Toste, F. D. *Science* **2015**, *350*, 1235-1238.
- (6) Zhang, Q.; Tiefenbacher, K. Nat. Chem. 2015, 7, 197-202.
- (7) Brown, C. J.; Toste, F. D.; Bergman, R. G.; Raymond, K. N. *Chem. Rev.* **2015**, *115*, 3012-3035.
- (8) Wang, Q. Q.; Gonell, S.; Leenders, S. H.; Durr, M.; Ivanovic-Burmazovic, I.; Reek, J. N. *Nat. Chem.* **2016**, *8*, 225-230.

- (9) Cullen, W.; Misuraca, M. C.; Hunter, C. A.; Williams, N. H.; Ward, M. D. *Nat. Chem.* **2016**, *8*, 231-236.
- (10) Cram, D. J.; Tanner, M. E.; Thomas, R. Angew. Chem., Int. Ed. 1991, 30, 1024-1027.
- (11) Warmuth, R. Angew. Chem., Int. Ed. 1997, 36, 1347-1350.
- (12) Warmuth, R.; Marvel, M. A. Chem. -Eur. J. 2001, 7, 1209-1220.
- (13) Mal, P.; Breiner, B.; Rissanen, K.; Nitschke, J. R. Science 2009, 324, 1697-1699.
- (14) Gibb, C. L.; Gibb, B. C. J. Am. Chem. Soc. 2006, 128, 16498-16499.
- (15) Liu, S.; Gan, H.; Hermann, A. T.; Rick, S. W.; Gibb, B. C. Nat. Chem. 2010, 2, 847-852.
- (16) Scarso, A.; Trembleau, L.; Rebek, J., Jr. J. Am. Chem. Soc. 2004, 126, 13512-13518.
- (17) Ajami, D.; Rebek, J., Jr. J. Am. Chem. Soc. 2006, 128, 15038-15039.
- (18) Ajami, D.; Rebek, J., Jr. Nat. Chem. 2009, 1, 87-90.
- (19) Gibb, C. L.; Gibb, B. C. Chem. Commun. 2007, 1635-1637.
- (20) Asadi, A.; Ajami, D.; Rebek, J., Jr. J. Am. Chem. Soc. 2011, 133, 10682-10684.
- (21) Choudhury, R.; Barman, A.; Prabhakar, R.; Ramamurthy, V. J. Phys. Chem., B **2013**, 117, 398-407.
- (22) Liu, S.; Russell, D. H.; Zinnel, N. F.; Gibb, B. C. J. Am. Chem. Soc. 2013, 135, 4314-4324.
- (23) Sacchettini, J. C.; Gordon, J. I.; Banaszak, L. J. J. Mol. Biol. 1989, 208, 327-339.
- (24) van den Berg, B.; Black, P. N.; Clemons, W. M., Jr.; Rapoport, T. A. *Science* **2004**, *304*, 1506-1509.
- (25) Zhang, K. D.; Ajami, D.; Gavette, J. V.; Rebek, J., Jr. *J. Am. Chem. Soc.* **2014**, *136*, 5264-5266.
- (26) Mosca, S.; Yu, Y.; Gavette, J. V.; Zhang, K. D.; Rebek, J., Jr. *J. Am. Chem. Soc.* **2015**, 137, 14582-14585.
- (27) Ko, Y. H.; Kim, H.; Kim, Y.; Kim, K. Angew. Chem., Int. Ed. 2008, 47, 4106-4109.
- (28) Wu, N. W.; Rebek, J., Jr. J. Am. Chem. Soc. 2016, 138, 7512-7515.
- (29) Shi, Q.; Masseroni, D.; Rebek, J., Jr. J. Am. Chem. Soc. 2016, 138, 10846-10848.
- (30) Shorthill, B. J.; Avetta, C. T.; Glass, T. E. J. Am. Chem. Soc. 2004, 126, 12732-12733.
- (31) Avetta, C. T.; Shorthill, B. J.; Ren, C.; Glass, T. E. J. Org. Chem. 2012, 77, 851-857.
- (32) Yazaki, K.; Sei, Y.; Akita, M.; Yoshizawa, M. Nat. Commun. 2014, 5, 5179.
- (33) Mosca, S.; Ajami, D.; Rebek, J., Jr. Proc. Natl. Acad. Sci. U. S. A. 2015, 112, 11181-11186.
- (34) Furuhashi, M.; Hotamisligil, G. S. Nature reviews. Drug discovery 2008, 7, 489-503.
- (35) Mozaffarian, D.; Aro, A.; Willett, W. C. Eur. J. Clin. Nutr. 2009, 63 Suppl 2, S5-21.
- (36) Momchilova, S. M.; Nikolova-Damyanova, B. M. Anal. Sci. 2012, 28, 837-844.
- (37) Gibb, C. L.; Gibb, B. C. J. Am. Chem. Soc. 2004, 126, 11408-11409.

- (38) Liu, S.; Whisenhunt-loup, S. E.; Gibb, C. L.; Gibb, B. C. Supramol. Chem. **2011**, 23, 480-485.
- (39) Gibb, C. L.; Gibb, B. C. J. Comput. Aided Mol. Des. 2014, 28, 319-325.
- (40) Sullivan, M. R.; Sokkalingam, P.; Nguyen, T.; Donahue, J. P.; Gibb, B. C. *J. Comput. Aided Mol. Des.* **2016**.
- (41) Carnegie, R. S.; Gibb, C. L.; Gibb, B. C. Angew. Chem., Int. Ed. 2014, 53, 11498-11500.
- (42) Sokkalingam, P.; Shraberg, J.; Rick, S. W.; Gibb, B. C. *J. Am. Chem. Soc.* **2016**, *138*, 48-51.
- (43) Jordan, J. H.; Gibb, B. C. Chem Soc Rev 2015, 44, 547-585.
- (44) Hiraoka, S.; Nakamura, T.; Shiro, M.; Shionoya, M. *J. Am. Chem. Soc.* **2010**, *132*, 13223-13225.
- (45) Suzuki, A.; Kondo, K.; Akita, M.; Yoshizawa, M. Angew. Chem., Int. Ed. **2013**, 52, 8120-8123.
- (46) Wang, K.; Sokkalingam, P.; Gibb, B. C. Supramol. Chem. 2016, 28, 84-90.
- (47) Rawling, T.; Duke, C. C.; Cui, P. H.; Murray, M. Lipids 2010, 45, 159-165.
- (48) Vedejs, E.; Fuchs, P. L. J. Am. Chem. Soc. 1973, 95, 822-825.
- (49) Barnett, J. W.; Gibb, B. C.; Ashbaugh, H. S. J. Phys. Chem. B 2016, 120, 10394-10402.
- (50) Tang, H.; de Oliveira, C. S.; Sonntag, G.; Gibb, C. L.; Gibb, B. C.; Bohne, C. *J. Am. Chem. Soc.* **2012**, *134*, 5544-5547.
- (51) Shih, K.-C.; Angelici, R. J. The Journal of Organic Chemistry 1996, 61, 7784-7792.
- (52) Sémon, E.; Ferary, S.; Auger, J.; Le Quéré, J. L. J. Amer. Oil Chem. Soc. 1998, 75, 101.
- (53) Gunstone, F. D.; Polard, M. R.; Scrimgeour, C. M.; Vedanayagam, H. S. Chem. Phys. Lipids 1977, 18, 115-129.